IEEE Access
Multidisciplinary | Rapid Review | Open Access Journal

Received January 16, 2020, accepted February 6, 2020, date of publication February 18, 2020, date of current version February 28, 2020.

Digital Object Identifier 10.1109/ACCESS.2020.2974770

Application of CUDA-Accelerated GO/PO Method in Calculation of Electromagnetic Scattering From Coated Targets

CHUNLEI DONG, LIXIN GUO, (Senior Member, IEEE), AND XIAO MENG
School of Physics and Optoelectronic Engineering, Xidian University, Xi'an 710071, China

Corresponding author: Chunlei Dong (xidiancld@163.com)

This work was supported in part by the National Natural Science Foundation of China under Grant 61871457, Grant 61701378, and Grant 61971338, in part by the Foundation for Innovative Research Groups of the National Natural Science Foundation of China under Grant 61621005, and in part by the Aeronautical Science Foundation of China under Grant 20172081009.

ABSTRACT In this study, fast calculations for the electromagnetic (EM) scattering of complex targets coated by radar absorbing materials have been reported. The Geometric Optics and Physical Optics (GO/PO) methods are combined with the modified surface reflection coefficient method, to solve the problem of EM scattering. Moreover, two acceleration techniques have been employed to improve the efficiency of computations. Firstly, the neighbor search technique is adopted to accelerate the ray tracing process in GO/PO. In this technique, an Octree structure is applied to divide the space into multiple subspaces, namely sub-nodes, where the efficiency of ray tracing can be improved through Morton code transform. In order to further reduce the computational time, parallel acceleration technique, based on GPU platform within the Compute Unified Device Architecture (CUDA) framework is introduced. Our proposed method has been verified from the nice correlation of simulated and multilevel fast multipole method (MLFMM) and CPU-based GO/PO methods. The runtime is compared with that of GO/PO method in serial model, responsible for a good speedup ratio. Finally, the influence of coating thicknesses and types of material on the EM scattering characteristics of the coated targets are also analyzed.

INDEX TERMS EM scattering, GO/PO method, CUDA, GPU, coated targets.

I. INTRODUCTION

Radar Cross Section (RCS) is an important feature in the fields of target detection and recognition. In order to reduce the RCS of targets, two main methods are adopted: changing the shape of targets and coating with radar absorbing materials [1]. With the rapid development of various advanced composite materials, a variety of lossy media have been widely used to reduce the RCS of targets. For example, the anisotropic medium not only absorbs the electromagnetic wave only but also concentrates the energy on the non-observing direction of the radar. This can be achieved by controlling the optical axis which can further reduce the RCS. Hence, the investigation of EM scattering characteristics of targets, coated with lossy media, has always been a hot issue.

The associate editor coordinating the review of this manuscript and approving it for publication was Giovanni Angiulli.

Currently, numerical and high-frequency approximation methods are mainly employed for the investigation of EM scattering. Numerical methods include the Method of Moment (MOM) [2], [3], the Finite Difference Time Domain (FDTD) [4], [5], and the Finite Element Method (FEM), etc. It is difficult to solve the EM scattering problem of electrical large complex targets through the numerical method. The reason behind this is the limited resources of computations. Therefore, we have adopted the high-frequency approximation methods.

In the last few decades, high-frequency approximation methods have been widely used for the investigation of EM scattering characteristics of electrical large targets. For example, the PO method is utilized to predict the RCS of simple smooth targets. However, only the first-order scattering is considered in PO method, so, that is why the computational accuracy is poor for the targets with complex structures. Multiple scattering of complex targets can

be effectively investigated by ray-tracing technique, such as GO/PO method [8]–[10]or Shooting and Bouncing Rays (SBR) method [11]–[13]. The computational cost of ray tracing process rapidly increases along with the increase in size of targets and frequency of incident waves. Acceleration techniques such as FPGA-based ray-box intersection algorithm [14], Octree or KD-tree based algorithm, and GPU-based parallel algorithms have been utilized to improve the efficiency of ray tracing [15]–[21]. Recently, we reported the neighbor search technique of Octree structure, to accelerate the ray tracing process [16]. In this technique, the intersecting facets with a ray of the adjacent nodes are searched from the bottom of Octree. This method uses structural characteristics of Octree and associates the sub-nodes of Octree with Morton codes. Finally, it reduces the consumption time by reducing the times of intersection test, between facets and rays.

This work is based on our previous report [16], where the EM scattering of complex targets, coated with radar absorbing materials is further investigated. In order to solve the EM scattering problem, the modified surface reflection coefficient is combined with the GO/PO method. In case of GO/PO method, the neighbor search technique of Octree structure is utilized to accelerate the ray tracing process. Besides, CUDA framework is employed to further improve the computational efficiency. This method utilizes powerful parallel computing capability of GPU and solves the ray tracing process in parallel mode. Meanwhile, a new method is proposed, where octree nodes are rearranged into an array with respect to the depth of node and number of nodes. The position of node in array is exactly the decimal transformation of the Morton code of the node. So, it means that the Morton code is unified with the octree structure and node storage locations. This new approach can make neighbor search technique more easily applied in CUDA framework.

The simulated results have a nice correlation with those of MLFMM, which confirm the validity of our method. The runtime is compared with that of GO/PO method in serial mode, where the computational time is greatly saved. Our simulated results indicate that CUDA-accelerated GO/PO algorithm can be excellently applied for the prediction of RCS of targets coated-radar absorbing materials. Finally, we have not only analyzed the EM scattering characteristics of coated targets at different coating materials and thicknesses, but also summarized the relationship between the performance of different materials and coating thickness.

II. EM SCATTERING OF THE COATING OBJECTS

GO/PO method can efficiently calculate the EM scattering of complex targets with large electrical size. Modifying the surface reflection coefficient method can be employed to calculate the scattering field of lossy medium-coated targets, which can improve the accuracy without high computational cost. Therefore, the combination of GO/PO method with modifying surface reflection coefficient method is beneficial for the investigation of EM scattering characteristics of the complex coated target with electrical large size. For the fast computations, the ray-tracing process is accelerated by the neighbor search technique. meanwhile, the GO/PO and modifying surface reflection coefficient method are parallelized by CUDA.

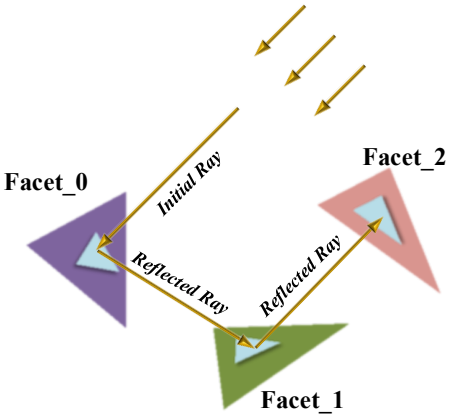

FIGURE 1. Ray tracing in the GO/PO method.

A. APPLICATION OF NEIGHBOR SEARCH TECHNIQUE FOR GO/PO

According to GO/PO method, multiple scattering between different facets of a target has a great influence on the EM scattering, which is shown in Fig.1. The path of reflected ray and electromagnetic intensity can be tracked by GO and the ray tracing technique. The far-scattered field of all illuminated surface elements is calculated by PO.

In GO/PO algorithm, ray tracing is an intricate and time-consuming process. Traditional ray-tracing acceleration techniques consist of Octree and KD-tree. From the division of space, the search area is gradually narrowed and the unnecessary intersection between facets and rays can be reduced. The efficiency of ray tracing is improved. In our previous work, we improved the ray tracing efficiency with the help of Octree neighbor search technique. The neighbor search algorithm predicts the intersecting Octree nodes with the bottom layer of rays. The process of intersecting tests can be reduced from combination of Morton coding and binary transformation technique. Therefore, we have applied this technique to improve the efficiency of GO/PO.

The process of GO/PO algorithm of the neighbor search technique is shown in Fig.2. In case of single ray, the position of the illuminated facet and reflected direction must be determined. In this paper, backward ray tracing has been employed to remove the shadow facets, which supposes that a ray is emitted from a facet in the opposite direction of the incident wave. If the ray is uncovered by other facets, then the facet is illuminated by the incident wave. Secondly, the neighbor search technique investigates the path of the adjacent nodes of ray. If there are no adjacent nodes, then this process terminates. And the intersection tests are carried out for the facets in adjacent nodes. If a face is illuminated by the reflected ray, then high-order ray tracing is carried out

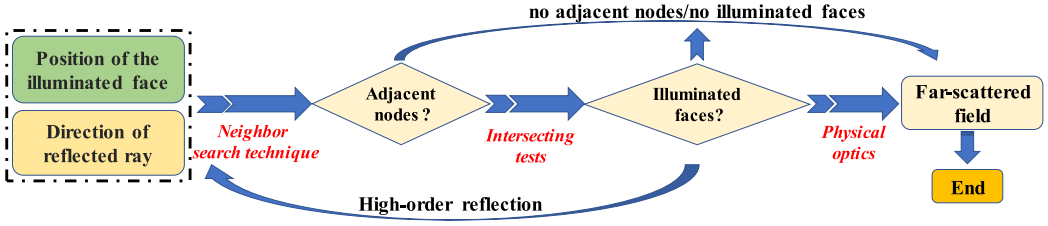

FIGURE 2. Octree structure.

until the condition of reflection order is achieved or there is no illuminated facet. Finally, the far-scattered fields of the illuminated facets are calculated by PO integral.

B. THE METHOD OF MODIFYING THE SURFACE REFLECTION COEFFICIENT

To calculate the EM scattering of single-layer medium surface, the Fresnel reflection coefficient R of the upper surface medium should be considered in PO integral equation. According to the theory of Modify Equivalent electromagnetic Current Algorithm (MECA) [22], the field of EM scattering can be carried out by decomposing the incident wave into horizontally polarized wave (TE) and vertically polarized wave (TM):

$$\boldsymbol{E}^{\text{inc}} = \boldsymbol{E}^{\text{inc}}_{\text{TE}} + \boldsymbol{E}^{\text{inc}}_{\text{TM}} = E^{\text{inc}}_{\text{TE}}\hat{\boldsymbol{e}}_{\text{TE}} + E^{\text{inc}}_{\text{TM}}\hat{\boldsymbol{e}}_{\text{TM}} \tag{1}$$

The reflection field can be expressed as

$$\begin{aligned} \boldsymbol{E}^{\text{r}}_{\text{TE}} &= E^{\text{inc}}_{\text{TE}} R_{\text{TE}}\hat{\boldsymbol{e}}_{\text{TE}} \\ \boldsymbol{E}^{\text{r}}_{\text{TM}} &= E^{\text{inc}}_{\text{TM}} R_{\text{TM}}\hat{\boldsymbol{s}}_{\text{TM}} = E^{\text{inc}}_{\text{TM}} R_{\text{TM}}(\hat{\boldsymbol{k}}_s \times \hat{\boldsymbol{e}}_{\text{TE}}) \end{aligned} \tag{2}$$

Therefore, the total electric field intensity of the upper half-space is:

$$\boldsymbol{E}^{\text{tot}} = \boldsymbol{E}^{\text{inc}} + R_{\text{TE}} E^{\text{inc}}_{\text{TE}}\hat{\boldsymbol{e}}_{\text{TE}} + R_{\text{TM}} E^{\text{inc}}_{\text{TM}}(\hat{\boldsymbol{k}}_s \times \hat{\boldsymbol{e}}_{\text{TE}}) \tag{3}$$

According to the relationship between magnetic and electric field, the total magnetic field intensity of the upper half-space can be obtained as:

$$\begin{aligned} \boldsymbol{H}^{\text{tot}} = &\frac{1}{\eta}\hat{\boldsymbol{k}}_{\text{inc}} \times \boldsymbol{E}^{\text{inc}} \\ &+ \frac{1}{\eta}[R_{\text{TE}} E^{\text{inc}}_{\text{TE}}(\hat{\boldsymbol{k}}_s \times \hat{\boldsymbol{e}}_{\text{TE}}) - R_{\text{TM}} E^{\text{inc}}_{\text{TM}}\hat{\boldsymbol{e}}_{\text{TE}}] \end{aligned} \tag{4}$$

Based on the assumption of physical optics, the equivalent electromagnetic current density of the surface can be expressed by the tangential component of the total electromagnetic field.

$$\boldsymbol{J} = \hat{\boldsymbol{n}} \times \boldsymbol{H}^{\text{tot}}\big|_s = \frac{1}{\eta}\left\{ \begin{array}{l} E^{\text{inc}}_{\text{TE}} \cos\theta_{\text{inc}}(1 - R_{\text{TE}})\hat{\boldsymbol{e}}_{\text{TE}} \\ +E^{\text{inc}}_{\text{TM}}(1 - R_{\text{TM}})(\hat{\boldsymbol{n}} \times \hat{\boldsymbol{e}}_{\text{TE}}) \end{array} \right\}\Big|_s \tag{5}$$

$$\boldsymbol{M} = -\hat{\boldsymbol{n}} \times \boldsymbol{E}^{\text{tot}}\big|_s = \left\{ \begin{array}{l} E^{\text{inc}}_{\text{TE}}(1 + R_{\text{TE}})(\hat{\boldsymbol{e}}_{\text{TE}} \times \hat{\boldsymbol{n}}) + \\ E^{\text{inc}}_{\text{TM}} \cos\theta_{\text{inc}}(1 + R_{\text{TM}})\hat{\boldsymbol{e}}_{\text{TE}} \end{array} \right\}\Big|_s \tag{6}$$

According to the physical optical integral formula, the far scattering field of the target surface can be expressed as

$$\begin{aligned} \boldsymbol{E}^{\text{s}} \approx &\frac{\text{j}}{2\lambda}\frac{\exp(-\text{j}kr)}{r} \\ &\cdot \int_s \left[\hat{\boldsymbol{s}} \times \boldsymbol{M} - \left(\hat{\boldsymbol{s}} \times \eta\boldsymbol{J} \times \hat{\boldsymbol{s}}\right)\right] \exp\left(\text{j}\boldsymbol{k}_s \cdot \boldsymbol{r}'\right) \text{d}s' \end{aligned} \tag{7}$$

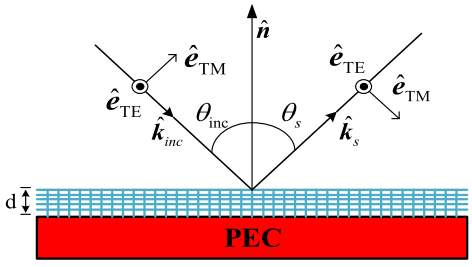

FIGURE 3. Schematic diagram of electromagnetic wave reflection.

where R_{TE} and R_{TM} are the reflection coefficient, $\hat{\boldsymbol{e}}_{\text{TE}}$ and $\hat{\boldsymbol{e}}_{\text{TM}}$ are the direction of polarization, $\hat{\boldsymbol{n}}$ is the normal direction of the plane, the wave impedance $\eta = \sqrt{\mu/(\varepsilon - j\sigma/\omega)}$, and the r' is the position vector at any point on the surface.

The calculated EM scattering field of the perfect conductor (PEC) lossy medium coated is shown in Fig.3. The equivalent electromagnetic current of the medium surface can be carried out from the modifying surface reflection coefficient.

According to electromagnetic wave propagation theory and boundary continuity relationship, the reflection coefficient of the medium coated on PEC can be expressed as follow [23]:

$$R_{\text{TE}} = \frac{Z_{\text{TE}} \cos\theta_i - 1}{Z_{\text{TE}} \cos\theta_i + 1} \tag{8}$$

$$R_{\text{TM}} = \frac{Z_{\text{TM}} - \cos\theta_i}{Z_{\text{TM}} + \cos\theta_i} \tag{9}$$

where Z_{TE} and Z_{TM} can be expressed as

$$\begin{aligned} Z_{\text{TE}} = &\frac{j\sqrt{\mu'_{11}\mu'_{33}}}{\sqrt{\mu'_{33}\varepsilon'_{22} - \sin^2\theta_i}} \\ &\cdot \tan(kd\sqrt{\mu'_{11}\varepsilon'_{22} - \mu'_{11}\sin^2\theta_i/\mu'_{33}}) \end{aligned} \tag{10}$$

$$\begin{aligned} Z_{\text{TM}} = &\frac{j\sqrt{\mu'_{22}\varepsilon'_{33} - \sin^2\theta_i}}{\sqrt{\varepsilon'_{11}\varepsilon'_{33}}} \\ &\cdot \tan(kd\sqrt{\mu'_{22}\varepsilon'_{11} - \varepsilon'_{11}\sin^2\theta_i/\varepsilon'_{33}}) \end{aligned} \tag{11}$$

k is the wavenumber in space, d is the thickness of coated layer. The permittivity and permeability of the medium can be expressed as

$$\varepsilon = \varepsilon_0 \cdot diag[\varepsilon'_{11}, \varepsilon'_{22}, \varepsilon'_{33}] \tag{12}$$

$$\mu = \mu_0 \cdot diag[\mu'_{11}, \mu'_{22}, \mu'_{33}] \tag{13}$$

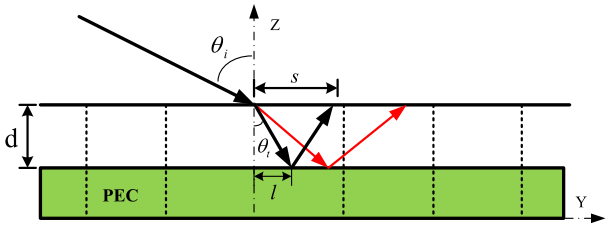

FIGURE 4. Schematic diagram of errors caused by ray tracing.

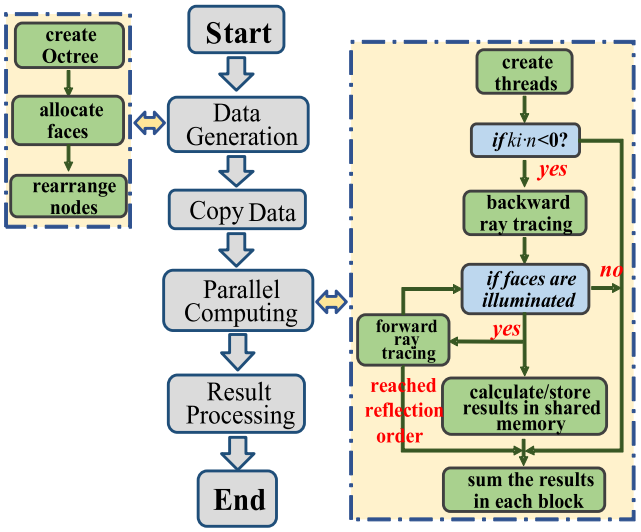

FIGURE 5. Flowchart of parallel computing.

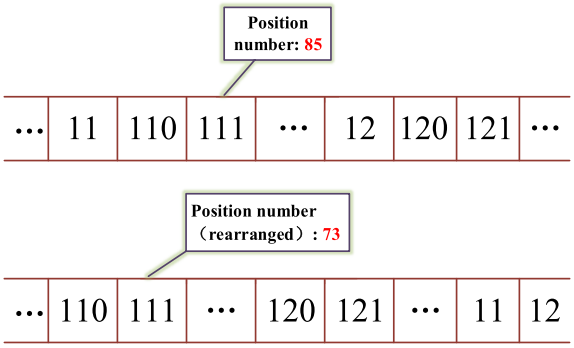

FIGURE 6. Schematic diagram of tree nodes arrangement.

By applying equations (8) and (9), J and M can be obtained which can calculate the far-field of the coated targets. On the other hand, GO tracks the field intensity of rays, and the reflection field intensity can be obtained from the modifying reflection coefficient.

The coated model is subdivided into many facets when the EM scattering fields are calculated by GO/PO. And the ray tracing is implemented on the surfacing of the coating. If the ray does not hit the target surface vertically, the position at which it hits the coated surface will be somewhat different from the position at which it hits the PEC surface, as shown in Fig. 4. The s is the size of facet. The offset $l = d * \tan\theta_t$. θ_t can be determined by Snell law. If $l > s$, the reflected ray from pec surface will illuminate other facets. Due to this phenomenon is ignored in this paper, when the thickness of the coating is more than the maximum thickness the inaccuracy will increase. So l should be less than s, so that $d_{\max} = s/\tan\theta_t$.

C. CUDA IMPLEMENTATION

GPU consists of a large number of computing cores, which can effectively support parallel computing. As a parallel computing architecture, CUDA can be conveniently accessed and use the computing resources of GPU. This is very suitable for completing tasks with high parallelism. As we know, ray tubes are independent of each other, so, the ray tracing can be easily implemented in GPU with a high degree of parallelism. As shown in Fig.5, CUDA-based accelerated ray tracing process can be divided into four parts, data generation, data copy, parallel computing, and processing result.

The first step is data generation which includes the creation of Octree and allocation of facets' information. This process is done on CPU because the CPU is more powerful for logical operations. After completing the allocation of facets' information, Octree nodes must be rearranged. So, the corresponding nodes are found from the Morton code. GPU can easily find and access the tree nodes if Morton codes directly transform into decimal number, which represents position of the nodes in array. It can be seen in Fig.6 that the value of Morton code transformation is equal to the number of positions of node.

In the second step, the data is copied to the GPU. Since the data exchange between GPU and CPU is a time-consuming process, so, the parameters are stored in an array and loaded to GPU from CPU in one time, which can avoid the multiple exchanges.

In third step, parallel calculations on GPU are performed. Initially, the scattering field of the illuminated faces, determined by backward ray tracing is calculated. This is followed by next order ray tracing. The forward tracing method and neighbor search technique are used to quickly find the intersecting of node with a ray, and the facets of intersecting nodes with a ray are tested. This process is repeated until the maximum reflection order is achieved or there is no intersecting face with the ray. Later on, the ray tracing process of the thread is completed. Global memory access is slowest among various memories. Hence, in attempting to accelerate the algorithm, the scattering field of each ray is stored in the shared memory, and the result of each thread of same block is summed up on GPU. Moreover, the result of each block is stored in global memory.

In fourth step, data is transferred back to CPU and further summed up. Due to the limited number of data in the tread blocks, the final sum has no performance loss on the CPU.

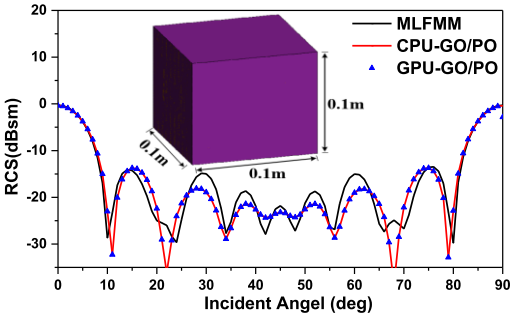

(a) Simulation results of a Cube coated by lossy medium

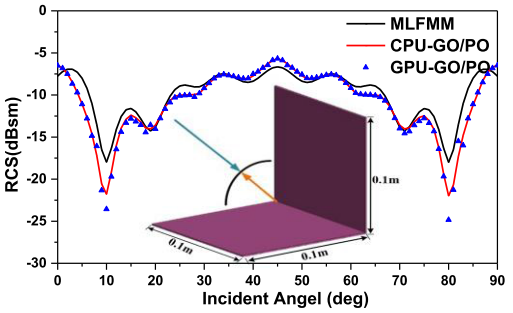

(b) Simulation results of a Dihedral coated by lossy medium

FIGURE 7. Comparison of simulation results.

III. RESULTS AND DISCUSSION

Our simulations are executed on a personal computer with an Intel Core I i5-6500 3.2 GHz CPU, 16G RAM, and NVIDIA GeForce GTX 1080Ti GPU. Programs are built and run under the Windows 10 64-bit operating system. Two examples are used to verify the efficiency of our method, and the runtime is compared.

A. VALIDATION

A cube and a dihedral coated lossy medium are chosen, to test the validity of the GPU-based GO/PO method. IN fig.7(a), the size of the cube is $0.1m \times 0.1m \times 0.1m$. the thickness of coating is 0.4mm. In case of an isotropic medium, $\varepsilon'_{11} = \varepsilon'_{22} = \varepsilon'_{33}$ is $(2, -14.2)$ and $\mu'_{11} = \mu'_{22} = \mu'_{33}$ is $(1, 0.0)$. Backscattering RCS with VV polarization is computed at 8GHz. The dihedral model is presented in Fig.7(b), whose length, width, and height are $l = 0.1$m, $w = 0.1$m and $h = 0.1$m, respectively. The thickness of coating is 1.2mm. In case of an isotropic medium, $\varepsilon'_{11} = \varepsilon'_{22} = \varepsilon'_{33}$ is $(4, -10.68)$ and $\mu'_{11} = \mu'_{22} = \mu'_{33}$ is $(2, -0.5)$. Backscattering RCS with HH polarization is computed at 10GHz. Both simulated results are compared with those obtained from MLFMM and CPU-based GO/PO method, shown in Fig.7(a) and (b). The incident angle varies from 0° to 90°, and the angular resolution is set to 1°. As depicted in Fig.7(a) and (b), a good agreement is achieved. The efficiency of our method for EM scattering of dihedral coated (by lossy medium) is verified (see TABLE 1).

In order to further verify the efficiency of our method, the simulated backscattering RCS and runtime performance of GPU-based GO/PO are compared with those of the CPU-based GO/PO method, and the results are shown in Fig.7 and TABLE 1. The model is presented in Fig.8(a). The thickness of coating is 1.2mm. The dielectric parameters are same as those of Fig.8(b). In Fig.8(b) the frequency of incident wave is 10GHz. The incident angle is 30°, and the incident azimuth angle varies from 0° to 180°, and the angular resolution is set to 0.2°. HH polarization is considered.

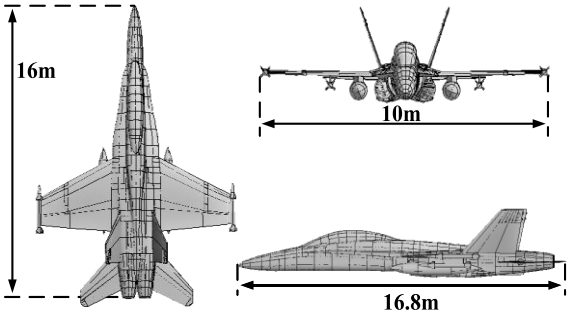

(a) Model of airplane

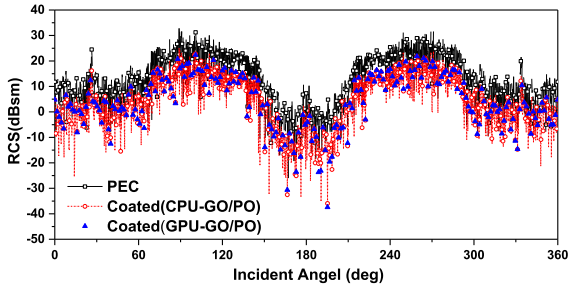

(b) Simulation results (10GHz, HH Polarization)

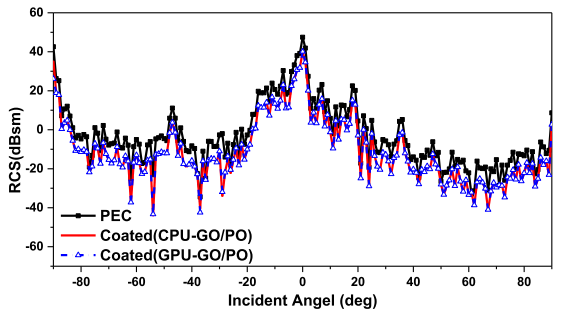

(c) Simulation results (18GHz, VV Polarization)

FIGURE 8. Comparison with traditional GO/PO method.

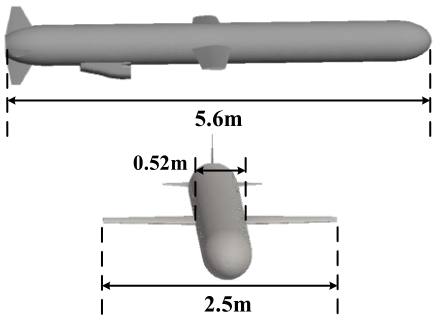

FIGURE 9. Model of missile.

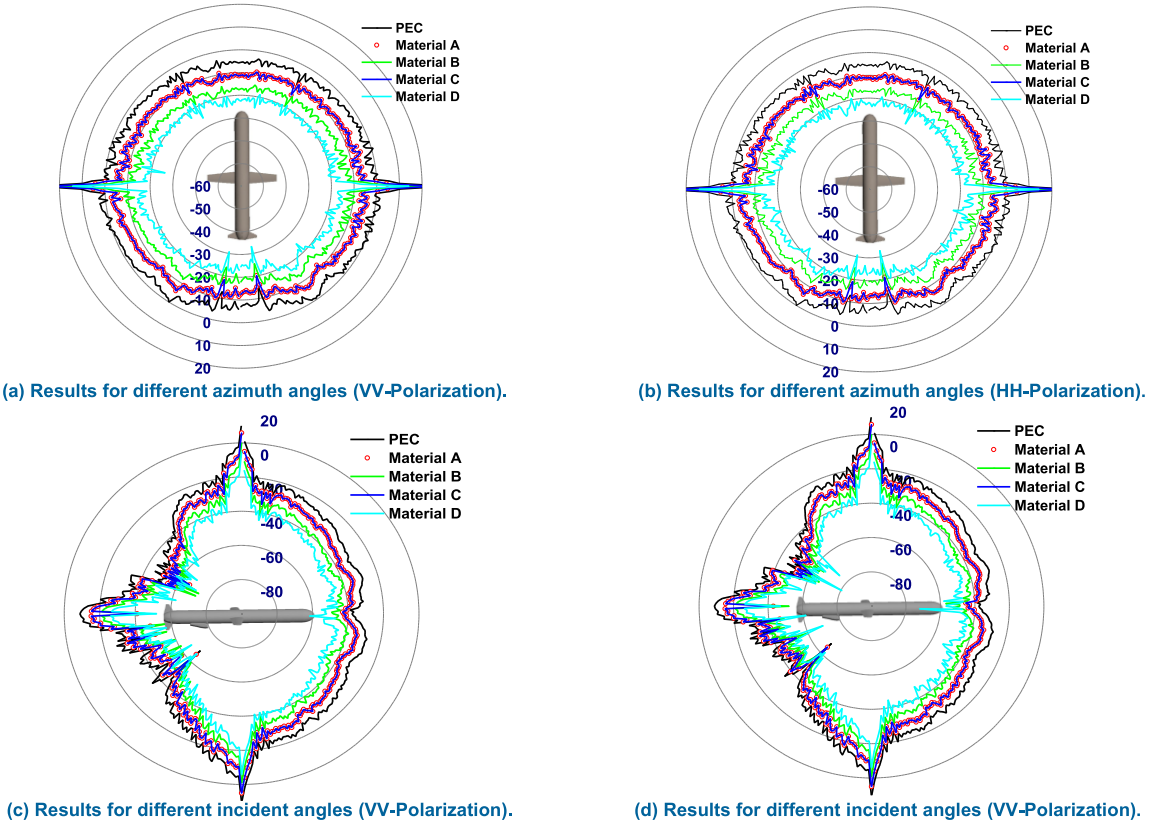

(a) Results for different azimuth angles (VV-Polarization).

(b) Results for different azimuth angles (HH-Polarization).

(c) Results for different incident angles (VV-Polarization).

(d) Results for different incident angles (VV-Polarization).

FIGURE 10. Results of different incident angles.

Moreover, in Fig.8(c), incident azimuth angle is 0°, and the incident angle varies from −90° to 90°, and the angular resolution is set to 1°. The frequency is 18GHz, and VV polarization is considered.

GPU-based GO/PO simulated results have nice correlations with the CPU-based GO/PO method, as shown in Fig.8(b) and (c). The computational time of GPU-based GO/PO is much shorter than that of CPU-based GO/PO method. Moreover, it should be noted that the speedup ratio can be improved with the increase in amount of computation. In parallel mode, the process of data exchange between CPU and GPU is time consuming, which account for a large proportion of the total time if computing process is fast. On the contrary, with the increases in amount of computation, the influence of data exchange will be weakened.

The efficiency of our method for EM scattering computation of targets coated by lossy medium is further demonstrated by compared the time Usage. In addition, the results of coated flight are lower than that of without coating, which shows the weakness of radar echoes in lossy medium.

B. EM SCATTERING CHARACTERISTICS OF COATED OBJECTS BY LOSSY MATERIAL

In this section, the GPU-based GO/PO and modifying surface reflection coefficient method is utilized to study the EM scattering characteristics of a coated missile, shown in Fig.9.

TABLE 1. Runtime comparison.

Examples	CPU-based GO/PO	GPU-based GO/PO	Speedup ratio
Fig.6(a)	6.4 (s)	0.69 (s)	9.2×
Fig.6(b)	39.1 (s)	1.3 (s)	29.3×
Fig.7(b)	730.3 (s)	14.54 (s)	50.2×
Fig.7(c)	419.3 (s)	7.96 (s)	52.7×

Four different materials are considered. Material A represents isotropic material, Material B represents positive uniaxial anisotropic material, Material C represents negative uniaxial anisotropic material, and Material D represents the nanomaterials. The parameters of these four materials are given as follows,

$$
\begin{aligned}
A &: \varepsilon_r = 27.32 - j4.58 \ \mu_r = 2.22 - j1.72 \\
B &: \varepsilon_r = diag[9.23 - j2.4, 9.23 - j2.4, 27.32 - j4.58] \\
&\quad \mu_r = diag[1.31 - j0.64, 1.31 - j0.64, 2.22 - j1.72] \\
C &: \varepsilon_r = diag[27.32 - j4.58, 27.32 - j4.58, 9.23 - j2.4] \\
&\quad \mu_r = diag[2.22 - j1.72, 2.22 - j1.72, 1.31 - j0.64] \\
D &: \varepsilon_r = 9 - j4.2 \ \mu_r = 1
\end{aligned}
$$

The backscattering RCS of the missile coated with different media at different angles is shown in Fig.10. The frequency of the incident wave is 10GHz, and the thickness of coating is 1.2mm. Both HH and VV polarization are considered. In Fig.10(a) and (b), the incident angle is

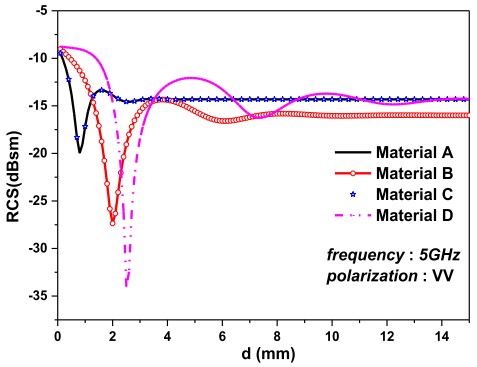

(a) The frequency of incident wave is 5GHz (VV-Polarization).

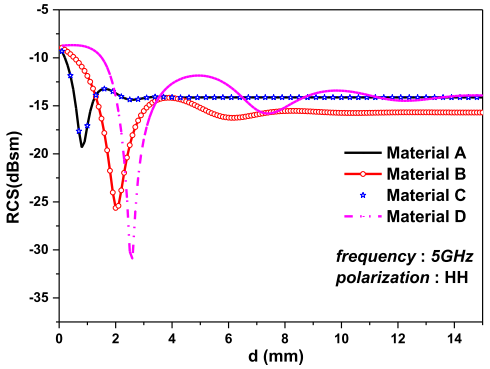

(b) The frequency of incident wave is 5GHz (HH-Polarization).

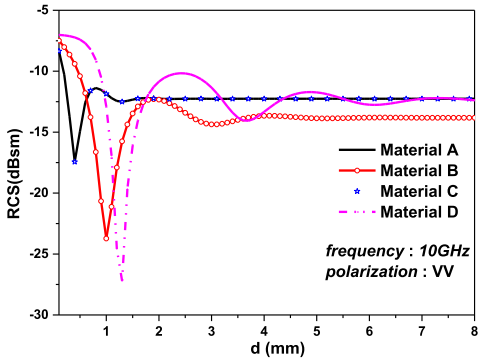

(c) The frequency of incident wave is 10GHz (VV-Polarization).

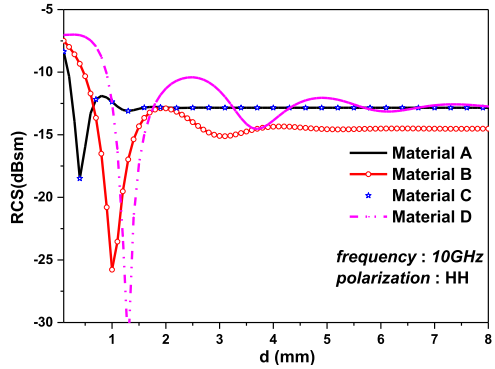

(d) The frequency of incident wave is 10GHz (HH-Polarization).

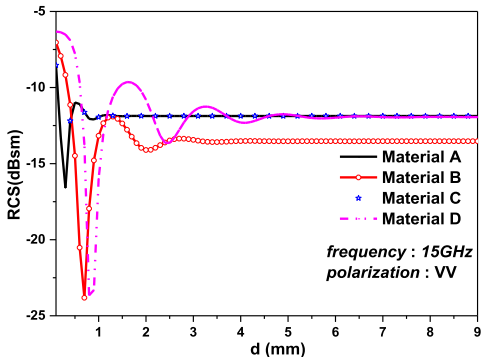

(e) The frequency of incident wave is 15GHz (VV-Polarization).

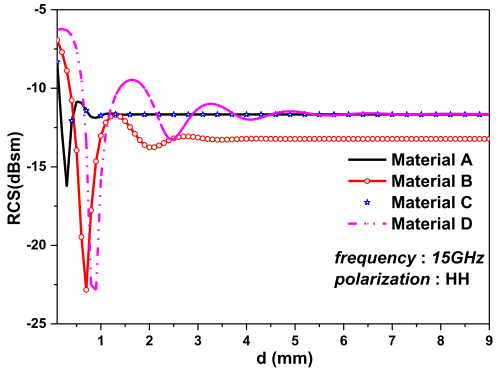

(f) The frequency of incident wave is 15GHz (HH-Polarization).

FIGURE 11. Results of different coating thickness.

30° and the incident azimuth angle varies from 0° to 360°, where the angular resolution is set as 1°. In Fig.10(c) and (d), the incident azimuth angle is 0° and the incident angle varies from 0° to 360°, where the angular resolution is set to 1°. The influence of isotropic material and negative uniaxial anisotropic material is similar, which indicates the absorption ability of negative uniaxial anisotropic media. And mainly depends on the transverse parameters of the medium. Moreover, the optical axis parameters have little influence on the absorption ability.

The influence of coating thickness on EM scattering is also investigated which is shown in Fig.11. The incident angle is set to 30° while the incident azimuth angle is taken 0°. Three different frequencies are considered. It is found that the backscattering RCS does not continuously decrease with the increase of thickness of the coating. This is due to the loss of electromagnetic waves in medium which increases with the increase of coating thickness. So, only the reflected

TABLE 2. Symbols and parameters.

symbol	Parameter	symbol	Parameter
ε_0	Permittivity of Vacuum	ε	Permittivity of Materials
ε_r	Relative Permittivity of Materials	ε'_{xx}	Permittivity on Principal axis of Anisotropic Materials
μ_0	Permeability of Vacuum	μ	Permeability of Materials
μ_r	Relative Permeability of Materials	μ'_{xx}	Permeability on Principal axis of Anisotropic Materials
diag[ ]	Diagonal Matrix	σ	Conductivity

waves of medium exist in the upper surface of target, if it is too thick. Thus, the reflection coefficient tends to be medium and the absorbing capacity will be stable with the increase in thickness. For all of these four materials, when the thickness of the coating is smaller than 0.02λ, the absorbing ability of the isotropic medium is superior, compared to that of others.

IV. CONCLUSION

In this paper, GO/PO method is combined with the modified reflection coefficient method for the investigation of EM scattering characteristics of coated targets. Meanwhile, the neighbor search and CUDA parallel acceleration techniques are adopted for the improve efficiency of computations. The validity of GPU-based GO/PO method is confirmed from the excellent correlation of MLFMM and CPU-based GO/PO method. Our simulated results have a good agreement which shows the improved computational capability. Moreover, the EM scattering of targets, coated by different radar absorbing materials, is also studied in detail. the results can be summarized as follow:

1) The influence of isotropic absorbing coating materials is almost same as that of negative uniaxial anisotropic absorbing coating materials.

2) At particular thickness, the absorbing capacity of different materials is very sensitive to thickness. However, when the thickness increases to a certain extent, the absorption capacity becomes stable. Different materials have different sensitivity ranges. With the increase of frequency, this sensitive range decreases.

3) When the thickness of coating is below 0.02λ, then isotropic materials have best absorbing capacity.

In general, the combined algorithm of GPU-based GO/PO and modified reflection coefficient, provides an efficient way for analysis of EM scattering characteristics of coated targets.

Some symbols representing medium parameters have been used many times in this paper. In order to definitely explain the meanings of these symbols, we summarize these symbols in Table 2.

REFERENCES

[1] E. F. Knott, J. Shaeffer, and M. Tuley, *Radar Cross Section*. Raleigh, NC, USA: SciTech Publishing, 2004.

[2] Z.-L. Liu, X. Wang, and C.-F. Wang, "A general MoM-PO hybrid framework for modelling complex antenna arrays mounted on extremely large platform (invited paper)," in *Proc. Int. Symp. Antennas Propag. (ISAP)*, 2013, pp. 48–51.

[3] H. Zhai and C. Liang, "A simple iterative method for considering multi-bounce in PO region of MoM-PO," *Microw. Opt. Technol. Lett.*, vol. 40, no. 2, pp. 110–112, Jan. 2004.

[4] K. Yee, "Numerical solution of initial boundary value problems involving Maxwell's equations in isotropic media," *IEEE Trans. Antennas Propag.*, vol. 14, no. 3, pp. 302–307, May 1966.

[5] J. Z. Lei, C. H. Liang, W. Ding, and Y. Zhang, "Study on MPI-based parallel modified conformal FDTD for 3-D electrically large coated targets by using effective parameters," *IEEE Antennas Wireless Propag. Lett.*, vol. 7, pp. 175–178, 2008.

[6] R. W. Clough, "The finite element method in plane stress analysis," in *Proc. 2nd ASCE Conf. Electron. Comput.*, Pittsburgh, PA, USA, 1960.

[7] M. M. Ilic and B. M. Notaros, "Higher order FEM-MoM domain decomposition for 3-D electromagnetic analysis," *IEEE Antennas Wireless Propag. Lett.*, vol. 8, pp. 970–973, 2009.

[8] W.-F. Huang, Z. Zhao, R. Zhao, J.-Y. Wang, Z. Nie, and Q. H. Liu, "GO/PO and PTD with virtual divergence factor for fast analysis of scattering from concave complex targets," *IEEE Trans. Antennas Propag.*, vol. 63, no. 5, pp. 2170–2179, May 2015.

[9] M. Zhang, Y. Zhao, J.-X. Li, and P.-B. Wei, "Reliable approach for composite scattering calculation from ship over a sea surface based on FBAM and GO-PO models," *IEEE Trans. Antennas Propag.*, vol. 65, no. 2, pp. 775–784, Feb. 2017.

[10] T.-Q. Fan and L.-X. Guo, "OpenGL-based hybrid GO/PO computation for RCS of electrically large complex objects," *IEEE Antennas Wireless Propag. Lett.*, vol. 13, pp. 666–669, 2014.

[11] H. Feng and X. Xu, "Simulation of bistatic scattering characteristics for multilayered dielectric targets," in *Proc. Sensor Signal Process. Defence Conf. (SSPD)*, London, U.K., Dec. 2017, pp. 1–5.

[12] T.-Q. Fan, L.-X. Guo, B. Lv, and W. Liu, "An improved backward SBR-PO/PTD hybrid method for the backward scattering prediction of an electrically large target," *IEEE Antennas Wireless Propag. Lett.*, vol. 15, pp. 512–515, 2016.

[13] F. Weinmann and J. Nitschkowski, "A SBR code with GO-PO for calculating scattered fields from coated surfaces," in *Proc. 4th Eur. Conf. Antennas Propag.*, 2010, pp. 1–4.

[14] P. Sundararajan and M. Y. Niamat, "FPGA implementation of the ray tracing algorithm used in the XPATCH software," in *Proc. MWSCAS*, Dayton, OH, USA, vol. 1, Nov. 2002, pp. 446–449.

[15] K.-S. Jin, T.-I. Suh, S.-H. Suk, B.-C. Kim, and H.-T. Kim, "Fast ray tracing using a space-division algorithm for RCS prediction," *J. Electromagn. Waves Appl.*, vol. 20, no. 1, pp. 119–126, Jan. 2006.

[16] C.-L. Dong, L.-X. Guo, X. Meng, and Y. Wang, "An accelerated SBR for EM scattering from the electrically large complex objects," *IEEE Antennas Wireless Propag. Lett.*, vol. 17, no. 12, pp. 2294–2298, Dec. 2018.

[17] M. Hapala and V. Havran, "Review: KD-tree traversal algorithms for ray tracing," *Comput. Graph. Forum*, vol. 30, no. 1, pp. 199–213, Mar. 2011.

[18] Y.-B. Tao, H. Lin, and H. J. Bao, "KD-tree based fast ray tracing for RCS prediction," *Prog. Electromagn. Res.*, vol. 81, pp. 329–341, 2008.

[19] S. Popov, J. Günther, H.-P. Seidel, and P. Slusallek, "Stackless KD-tree traversal for high performance GPU ray tracing," *Comput. Graph. Forum*, vol. 26, no. 3, pp. 415–424, Sep. 2007.

[20] A. S. Glassner, "Space subdivision for fast ray tracing," *IEEE Comput. Grap. Appl.*, vol. CGA-4, no. 10, pp. 15–24, Oct. 1984.

[21] P.-B. Wei, M. Zhang, W. Niu, and W.-Q. Jiang, "GPU-based combination of GO and PO for electromagnetic scattering of satellite," *IEEE Trans. Antennas Propag.*, vol. 60, no. 11, pp. 5278–5285, Nov. 2012.

[22] Y. Tao, H. Lin, and H. Bao, "GPU-based shooting and bouncing ray method for fast RCS prediction," *IEEE Trans. Antennas Propag.*, vol. 58, no. 2, pp. 494–502, Feb. 2010.

[23] C. Y. Kee and C.-F. Wang, "Efficient GPU implementation of the high-frequency SBR-PO method," *IEEE Antennas Wireless Propag. Lett.*, vol. 12, pp. 941–944, 2013.

[24] C. Y. Kee, C.-F. Wang, and T. T. Chia, "Optimizing high-frequency PO-SBR on GPU for multiple frequencies," in *Proc. IEEE 4th Asia–Pacific Conf. Antennas Propag. (APCAP)*, Kuta, Indonesia, Jun. 2015, pp. 132–133.

[25] J. G. Meana, J. Á. Martinez-Lorenzo, F. Las-Heras, and C. Rappaport, "Wave scattering by dielectric and lossy materials using the modified equivalent current approximation (MECA)," *IEEE Trans. Antennas Propag.*, vol. 58, no. 11, pp. 3757–3761, Nov. 2010.

[26] S. Tian, Z. Li, and C. Gu, "Equivalent electromagnetic currents on infinite stratified homogeneous bianisotropic media backed by a PEC layer," *Appl. Comput. Electromagn. Soc. J.*, vol. 1, no. 5, p. 3, 2011.

CHUNLEI DONG received the B.S. degree in electronic information science and technology from Xidian University, Xi'an, China, in 2015, where he is currently pursuing the Ph.D. degree in radio physics with the School of Physics and Optoelectronic Engineering.

His research has been on the composite scattering from 3-D large-scale rough sea surface with targets and SAR imaging.

LIXIN GUO (Senior Member, IEEE) received the M.S. degree in radio science from Xidian University, Xi'an, China, and the Ph.D. degree in astrometry and celestial mechanics from the Chinese Academy of Sciences, China, in 1993 and 1999, respectively.

From 2001 to 2002, he was a Visiting Scholar with the School of Electrical Engineering and Computer Science, Kyungpook National University, South Korea. He has also held appointments as a Visiting Professor at the d'Energetique des Systemes et Precedes (LESP), University of Rouen, France, and the Faculty of Engineering and Physical Sciences, The University of Manchester, U.K. He is currently a Professor and the Head of the School of Science, Xidian University, China. His research interests include electromagnetic wave propagation and scattering in complex systems, computational electromagnetic, and fractal electrodynamics.

Prof. Guo is a Senior Member of Chinese Institute of Electronics (CIE) and a Fellow of Physics Institute of Shaanxi Province, China.

XIAO MENG received the B.S. degree in electronic information science and technology and the Ph.D. degree in radio science from Xidian University, Xi'an, China, in 2011 and 2016, respectively.

She is currently a Teacher at Xidian University, China. Her research has been on the composite scattering from 3-D large-scale rough sea surface with targets and GPU high-performance computing in remote sensing.